

A spline for your saddle

Rebecca Granot and Roi Baer

Citation: *J. Chem. Phys.* **128**, 184111 (2008); doi: 10.1063/1.2916716

View online: <http://dx.doi.org/10.1063/1.2916716>

View Table of Contents: <http://aip.scitation.org/toc/jcp/128/18>

Published by the [American Institute of Physics](#)

A spline for your saddle

Rebecca Granot and Roi Baer^{a)}

*Institute of Chemistry and the Fritz Haber Center for Molecular Dynamics,
the Hebrew University of Jerusalem, Jerusalem 91904, Israel*

(Received 11 February 2008; accepted 3 April 2008; published online 14 May 2008)

Pinpointing extrema on a multidimensional hypersurface is an important generic problem with a broad scope of application in statistical mechanics, biophysics, chemical reaction dynamics, and quantum chemistry. Local minima of the hypersurface correspond to metastable structures and are usually the most important points to look for. They are relatively easy to find using standard minimizing algorithms. A considerably more difficult task is the location of saddle points. The saddle points most sought for are those which form the lowest barriers between given minima and are usually required for determining rates of rare events. We formulate a path functional minimum principle for the saddle point. We then develop a cubic spline method for applying this principle and locating the saddle point(s) separating two local minima on a potential hypersurface. A quasi-Newton algorithm is used for minimization. The algorithm does not involve second derivatives of the hypersurface and the number of potential gradients evaluated is usually less than 10% of the number of potential evaluations. We demonstrate the performance of the method on several standard examples and on a concerted exchange mechanism for self-diffusion in diamond. Finally, we show that the method may be used for solving large constrained minimization problems which are relevant for self-consistent field iterations in large systems. © 2008 American Institute of Physics. [DOI: 10.1063/1.2916716]

I. INTRODUCTION

A detailed understanding of elementary chemical reactions, i.e., determining the mechanisms and rates, can be gained in principle directly from the relevant Born—Oppenheimer potential hypersurface.^{1,2} However, in all but the simplest cases, this is a multidimensional conglomerate and is much too intricate for direct human interpretation, without additional computational steps. In principle, molecular dynamics can be used to gain some insight but in the case of chemical reactions, this by itself is seldom useful because these are extremely rare events.

A topographical approach is often the only practical way to obtain the essential characteristics of a chemical reaction. Chemically, the most important “topographical features” are the deep local minima, representing stable and metastable chemical species. Next in line come the saddle points, connecting adjacent local minima, through which the dominant chemically reactive paths pass. A saddle point can be described by a limiting process. Consider all possible paths leading from the reactants local minimum to that of the products. Each such path can be labeled by a number: The maximal value of the potential energy occurring as one travels along it from reactants to products. One can now focus on the path (there could be more than one) that has the smallest such maximal potential and locate the point along it of maximal potential. This point is the *saddle point*. In the direction of the tangent this point is a local maximum, and in any perpendicular direction it must be nonincreasing (otherwise, one can slightly distort the path in such a direction and ob-

tain a path of smaller maximal potential). The gradient of the potential function at the saddle point is therefore zero. Also, the Hessian of the potential surface at the saddle point is nondefinite: Some of its eigenvalues are positive while the others are negative (typically, only one eigenvalue is negative and it points in the direction of the tangent). Once the location of the saddle point and its potential is determined, one can make some rough estimates concerning the reaction rate, using, for example, transition state theory,^{3,4} or some of the more elaborate variants,^{5–9} or other methods.¹⁰

An additional significant topological feature is the concept of minimum energy path. If one has already determined a simple saddle point, one can reasonably easily slide from it in two opposite directions along the instantaneous steepest descent direction until a local minimum is reached on each side. The paths thus taken are the two parts of the minimum energy paths (MEPs) or reaction coordinate (other names exist as well).^{11–14} Mathematically, the MEP is a path connecting two local minima having the property that its tangent is forever parallel to the local gradient of the surface. The point of highest potential energy along the MEP is the saddle point. Numerical methods have been developed for efficient and stable “steepest descent sliding” along the MEP down to the minimum.^{15,16}

The importance of MEPs and saddle points in chemical reaction dynamics has led to the development of a wealth of methods for locating them. Many of the concepts and ideas were laid down already in early work, which was based on a search of the saddle point.^{17–23} A different approach to the problem consisted of paths represented by a chain of discrete configurations.^{24,25} The configurations were iteratively improved so as to bring them, in some sense, to a path similar

^{a)}Electronic mail: roi.baer@huji.ac.il.

as possible to the MEP. This approach inspired a large body of subsequent work in which each configuration along the path was augmented in a way that eliminates the nontangential component of the local gradient.^{26–28} Within these chain of configurations or string approaches, many new and interesting papers have emerged.^{29–33} Several excellent reviews cover the resulting work.^{34–41}

The importance of finding saddle points is not limited to chemical reaction dynamics or statistical mechanics. An efficient method of saddle point search is of broad importance for all problems that require constrained minimization. Constrained minimization problems can be mapped onto saddle point searches using Lagrange multipliers.⁴² One important example is in quantum chemistry, where the search for a Kohn–Sham or Hartree–Fock self-consistent field (SCF) solution can be done by minimization of the energy under the constraints of orthonormal orbitals.⁴³

In this paper we use a string method for locating a saddle point on a multidimensional hypersurface. We do not try to use the method for determining the MEP directly, because once the saddle point is determined, one can use a variety of existing methods for finding the MEP. As a demonstration of the potential utility of our method for a general optimization problem, we solve a simple constrained minimization problem.

II. MINIMUM PRINCIPLE FOR THE SADDLE POINT

Extremal points, such as minima and saddle points, are conventionally defined using the differential properties of the potential energy surface (PES).⁴⁴ In this section we take a different point of view which is necessary for understanding the method. We define saddle points using a *path functional approach*. This allows us to formulate a minimum principle for the saddle point. Such a principle is then used in the next section for locating the saddle point.

Consider a system of particles with coordinates $\mathbf{q}=(q^1, \dots, q^N)$ and a N -dimensional potential hypersurface $v(\mathbf{q})$. In future applications, it may be useful to consider the nature of the coordinates (whether angular or Cartesian). Here, however, we simply treat the coordinates as Cartesian. Suppose we are given two configurations, the reactants \mathbf{q}_ρ and the products \mathbf{q}_π . These are assumed here to be local minima of the potential, so the gradient vector $\partial_i v = -F_i$ vanishes and the $N \times N$ Hessian matrix of second derivatives $\partial_i \partial_j v$ is positive definite at these points. A smooth path \mathbf{q} connecting the reactants and products is a smooth series of points $\mathbf{q}(t)$ parameterized by a parameter $0 \leq t \leq 1$, with $\mathbf{q}(0) = \mathbf{q}_\rho$ and $\mathbf{q}(1) = \mathbf{q}_\pi$. Note that we use the symbol \mathbf{q} in several contexts: \mathbf{q} is the entire path and $\mathbf{q}(t)$ is a point on it. By “smooth” we mean that the first and second derivatives $\dot{\mathbf{q}}(t)$ and $\ddot{\mathbf{q}}(t)$ exist and are continuous at any t . Any path \mathbf{q} is a plausible chain of events leading from the reactants to the products.

Let us now discuss how we find saddle points on the hypersurface using paths. First, we define an energy functional $v_{\max}[\mathbf{q}]$ as the maximal energy along the path \mathbf{q} , mathematically,

$$v_{\max}[\mathbf{q}] \equiv \max_{0 \leq t \leq 1} v(\mathbf{q}(t)). \quad (2.1)$$

Let $t_{\max}[\mathbf{q}]$ denote the time at which the potential maximum is obtained (if it is obtained at several times let t_{\max} be the earliest),

$$v_{\max}[\mathbf{q}] = v(\mathbf{q}(t_{\max}[\mathbf{q}])). \quad (2.2)$$

As $v(\mathbf{q}(t))$ obtains its maximum at $t = t_{\max}$, the time derivative of $v(\mathbf{q}(t))$ must be zero and, therefore,

$$0 = \left. \frac{d}{dt} v(\mathbf{q}(t)) \right|_{t=t_{\max}} = \nabla v(\mathbf{q}(t_{\max})) \cdot \dot{\mathbf{q}}(t_{\max}). \quad (2.3)$$

The functional derivative of $v_{\max}[\mathbf{q}]$ is calculated from

$$\frac{\delta v_{\max}[\mathbf{q}]}{\delta \mathbf{q}(t)} = \nabla v(\mathbf{q}(t_{\max}[\mathbf{q}])) \cdot \left[\frac{\delta \mathbf{q}(t_{\max})}{\delta \mathbf{q}(t)} + \dot{\mathbf{q}}(t_{\max}) \frac{\delta t_{\max}[\mathbf{q}]}{\delta \mathbf{q}(t)} \right]. \quad (2.4)$$

Using Eq. (2.3) and the obvious,

$$\frac{\delta q_i(t_{\max})}{\delta q_j(t)} = \delta_{ij} \delta(t - t_{\max}), \quad i, j = 1, \dots, N, \quad (2.5)$$

we find

$$\frac{\delta v_{\max}[\mathbf{q}]}{\delta \mathbf{q}(t)} = \nabla v(\mathbf{q}(t)) \delta(t - t_{\max}) = \nabla v(\mathbf{q}(t_{\max}[\mathbf{q}])) \delta(t - t_{\max}) \quad (2.6)$$

Thus, the functional derivative of v_{\max} is different from zero only at the maximum (when $t = t_{\max}$) and then it is proportional to the gradient of the potential at the maximum.

Now we minimize v_{\max} , i.e., select the paths with the smallest value of v_{\max} . Suppose that \mathbf{q}_1 is one such a path. Obviously,

$$v_{\max}[\mathbf{q}_1] = \min_{\mathbf{q}} v_{\max}[\mathbf{q}]. \quad (2.7)$$

We denote also the saddle point \mathbf{q}_{sp} as a point of highest potential,

$$\mathbf{q}_{\text{sp}} = \mathbf{q}_1(t_{\max}[\mathbf{q}_1]). \quad (2.8)$$

Because \mathbf{q}_1 minimizes v_{\max} , we must have, for all t $\left. \frac{\delta v_{\max}}{\delta \mathbf{q}(t)} \right|_{\mathbf{q}_1} = 0$. Thus, using Eq. (2.6), the gradient of the potential at the saddle point vanishes,

$$\nabla v(\mathbf{q}_{\text{sp}}) = 0 \quad (2.9)$$

This shows that the way we defined the saddle point indeed leads to an extremal point of the potential hypersurface.

One of the characteristics of the saddle point is that the Hessian is not positive nor negative definite. Clearly the \mathbf{q}_{sp} being a point of $\mathbf{q}_1(t)$, which is a *minimizer* of v_{\max} , cannot be a local maximum of the surface. We now show that it cannot be a local minimum and, therefore, a true saddle point. Indeed, consider the equalities

$$\frac{d}{dt}v(\mathbf{q}_1(t)) = \nabla v(\mathbf{q}_1(t)) \cdot \dot{\mathbf{q}}_1(t) \quad (2.10)$$

$$\frac{d^2}{dt^2}v(\mathbf{q}_1(t)) = \nabla(\nabla v(\mathbf{q}_1(t)) \cdot \dot{\mathbf{q}}_1(t)) \cdot \dot{\mathbf{q}}_1(t) + \nabla v(\mathbf{q}_1(t)) \cdot \ddot{\mathbf{q}}_1(t).$$

At the saddle point $\nabla v(\mathbf{q}_{\text{sp}}) = 0$, so

$$\frac{d^2}{dt^2}v(\mathbf{q}_1(t_{\text{max}})) = \dot{\mathbf{q}}_1(t_{\text{max}})^T \vec{\mathbf{H}} \dot{\mathbf{q}}_1(t_{\text{max}}). \quad (2.11)$$

Where $\vec{\mathbf{H}} = \nabla \nabla v_{\text{max}}(\mathbf{q}_{\text{sp}})$. Since $v(\mathbf{q}(t))$ obtains a maximum at t_{max} , the second time derivative on the left hand side of Eq. (2.11) must be negative. Thus,

$$\dot{\mathbf{q}}_1(t_{\text{max}})^T \vec{\mathbf{H}} \dot{\mathbf{q}}_1(t_{\text{max}}) < 0. \quad (2.12)$$

This shows that $\vec{\mathbf{H}}$ must have negative eigenvalues and is thus not positive definite.

III. A SPLINE FOR THE SADDLE

The path $\mathbf{q}(t)$ that minimizes v_{max} passes through the saddle point at \mathbf{q}_{sp} . Let us exploit this fact in the following way. Using cubic splines, we can define a family of smooth paths that can be easily manipulated numerically. Within this family, we search for a minimum of v_{max} . This will yield an approximation for the saddle point. The quality of the approximation can be checked by calculating the norm of the gradient $g = \|\nabla v_{\text{max}}\|$, which is exactly 0 at the saddle point. A spline can be made rigid or flexible, by determining the number of anchor points (see below). By increasing the flexibility the saddle point can be approached. In practice, only a small number of anchor points is necessary.

Let us now discuss the method in more detail. We use smooth cubic splines⁴⁵ (one in each dimension) for representing the paths. It is well known that splines are flexible and are easily handled numerically. A spline is a path formed by P polynomials connecting sequentially at $P+1$ anchor points $\mathbf{Q}_0, \dots, \mathbf{Q}_P$. Specifically, the spline path $\tilde{\mathbf{q}}(t)$ passes through the anchor points \mathbf{Q}_p at times $t_p = p/P$, $p=0, \dots, P$,

$$\tilde{\mathbf{q}}(t_p) = \mathbf{Q}_p. \quad (3.1)$$

Any pair of sequential anchor points of the spline are connected by cubic polynomials (in each dimension) of the parameter t . These are constructed in such a way as to ensure second order smoothness: The path $\tilde{\mathbf{q}}(t)$, its tangent, the velocity $\dot{\tilde{\mathbf{q}}}(t)$, and the acceleration $\ddot{\tilde{\mathbf{q}}}(t)$ are continuous for all t —including at the anchor points. A spline representation of an analytical function converges as P^{-4} . So splines form a high order representation of any given smooth path.

For splines connecting local minima as ours, we choose the initial and final anchors as the reactant and product configurations, i.e.,

$$\mathbf{Q}_0 = \tilde{\mathbf{q}}(0) \equiv \mathbf{q}_\rho, \quad \mathbf{Q}_P = \tilde{\mathbf{q}}(1) \equiv \mathbf{q}_\pi. \quad (3.2)$$

Furthermore, the splines are taken to be “natural splines,” i.e., they have zero “acceleration” at the local minima,

$$\ddot{\tilde{\mathbf{q}}}(0) = \ddot{\tilde{\mathbf{q}}}(1) = 0. \quad (3.3)$$

This is not necessary, but something has to be assumed for \tilde{q} at the endpoints, and this is natural. A useful description of splines and their construction appears in Numerical Recipes.⁴⁶

Suppose we have a spline passing near a saddle point. One can then optimize the location of the anchor points \mathbf{Q}_p ($p=1, \dots, P-1$) such that the maximal potential function,

$$\tilde{v}_{\text{max}}[\mathbf{Q}_1, \dots, \mathbf{Q}_{P-1}] = v_{\text{max}}[\tilde{\mathbf{q}}] = v(\tilde{\mathbf{q}}(t_{\text{max}})), \quad (3.4)$$

is minimized. For any spline $\tilde{\mathbf{q}}$, the maximal potential $v_{\text{max}}[\tilde{\mathbf{q}}]$ and the time at which it is obtained, $t_{\text{max}}[\tilde{\mathbf{q}}]$, can both be determined by efficient one-dimensional maximization methods as described below.

Similar arguments leading to Eqs. (2.4) and (2.6) can be invoked to show that the gradient of $\tilde{v}(\mathbf{Q}_1, \dots, \mathbf{Q}_{P-1})$ is given by

$$\frac{\partial \tilde{v}_{\text{max}}}{\partial Q_p^d} = \frac{\partial v(\tilde{\mathbf{q}}(t_{\text{max}}))}{\partial q^n} J_d^{n,p}, \quad p=1, \dots, P-1, \quad (3.5)$$

$$d=1, \dots, N,$$

where we use the convention that repeated indices are summed over. In Eq. (3.5), the Jacobian is defined as

$$J_d^{n,p} \equiv \frac{\partial \tilde{q}^n(t_{\text{max}})}{\partial Q_p^d}, \quad n=1, \dots, N. \quad (3.6)$$

We see from Eqs. (3.5) and (3.6) that the gradient of the function to be minimized, $\tilde{v}_{\text{max}}(\mathbf{Q}_1, \dots, \mathbf{Q}_P)$ is established, without the need to compute Hessians.

Using the gradient of \tilde{v}_{max} , Eq. (3.5), a gradient-based minimizing algorithm may be established to find the approximate saddle point. We found that the general purpose quasi-Newton limited memory Broyden-Fletcher-Goldfarb-Shanno (BFGS) method⁴⁷ works extremely well for this purpose.

We are now summarizing two important numerical steps of the method:

- (1) The calculation of v_{max} for any given cubic spline is done as follows. In order to find the global maximum, we first compute the potential at $K \times P$ points equally spaced in time along the spline curve (typically we take $K=4$). Then select the highest potential point, say at $t = k/KP$. Now assume that the global maximum occurs inside the time interval $[(k-1)/KP, (k+1)/KP]$. The next step is to converge within this interval to the maximum. This is done using Brent's method, which enjoys fast (superlinear) convergence requiring no potential gradients. Because the work done in this algorithm is proportional to K , it is important to develop a method for setting K to a small as possible value, without missing the global maximum. Work on this issue is along the way.
- (2) The optimal location of the spline anchor points is determined by minimizing v_{max} using the Limited Memory BFGS quasi-Newton method,⁴⁷ based on the gradient of the potential at t_{max} . This method too was found to be super linear and highly efficient.

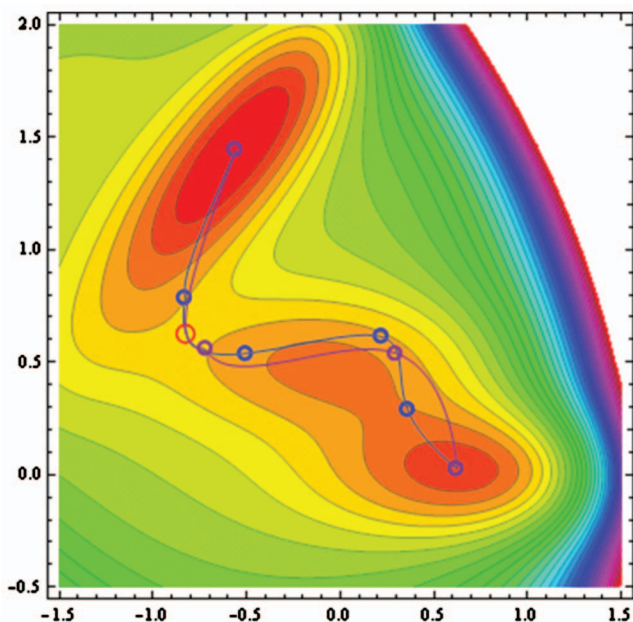


FIG. 1. (Color) $P+1=4$ and $P+1=6$ anchor point spline paths minimizing v_{\max} . The splines start and end at the same points and both pass through the saddle-point (center of the red circle). Otherwise, the paths are generally different.

The method thus suggested is variational, does not require Hessian evaluation, and is well suited for small and large problems. The success relies on a reasonable guess path that passes sufficiently close to the saddle point.

IV. EXAMPLES

A. The Müller-Brown potential

We demonstrate the method on the popular benchmark, the Müller-Brown (MB) potential surface⁴⁸ (see Fig. 1). This system is also discussed in some detail in Ref. 30. The two-dimensional MB potential surface consists of two main minima with an intermediate minimum that deflects the path at an angle. The lower minimum (“reactants”) is at $r_1 = (-0.5582, 1.44173)$ with $V_{\min} = -146.70$ and the second (“products”) is at $r_2 = (0.6235, 0.0280)$ with $V_{\min} = -108.17$. We start with a $P+1=4$ point spline, initially just a straight line connecting the reactants and products.

After converging to the minimum of $\tilde{v}(\mathbf{Q}_1, \dots, \mathbf{Q}_P)$, we can test the quality of $\tilde{\mathbf{q}}(t_{\max})$ by calculating \tilde{F}_{sp} .

The converged spline path has no physical meaning except for its ability to achieve a minimal v_{\max} . This is evident in Fig. 1 where two splines (differing in the number of anchor points) are shown. The paths are noticeably different but they both pass very close to the saddle point. In Fig. 2 we show the gradient at the saddle point \tilde{F}_{sp} , as a function of numerical work as the minimizing algorithm develops. The numerical work is measured by the number of potential evaluations (the number of gradient evaluations is about 10% of the number of energy evaluations). Interestingly, the efficiency is not necessarily a monotonic function of the number of anchor points $P+1$. This will be seen in the LEPS problem as well.

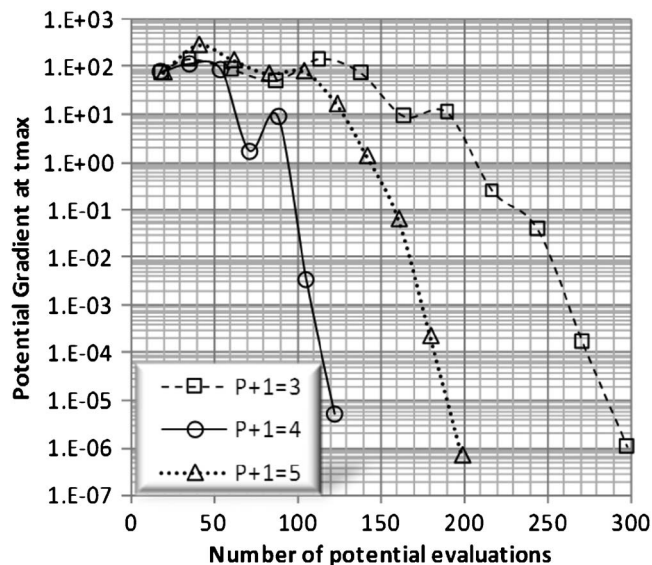


FIG. 2. The gradient at the approximated saddle point of the Müller-Brown potential as a function of number of potential evaluations during the LBFGS minimizing iterations. Splines with 3, 4, and 5 anchor points are shown.

The high precision of our method enables us to minimize the gradient to less than 10^{-6} . At such high precision of the gradient, we expect the energy to be of ~ 12 significant digits: $V_{\text{sp}} = -40.664843509$. We can also determine the position of the saddle point to 7–8 significant digits: $\mathbf{r}_{\text{sp}} = (-0.82200156, 0.62431280)$.

The efficiency of this method is studied in Fig. 3, where the approach to the saddle point is shown as a function of the number of potential and gradient evaluations. We compare our results to that of other methods for this benchmark system published in Ref. 30. The fact that we use a spline and search for v_{\max} along a smooth path enables us to quickly converge to the saddle point even without actually having the sampling points there.

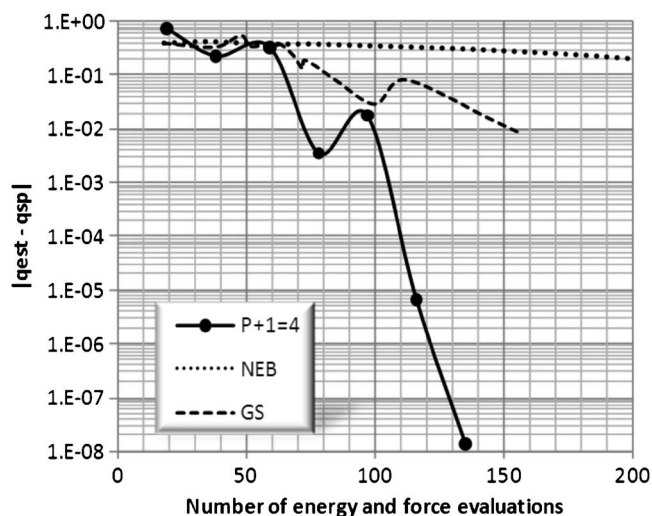


FIG. 3. The rate of convergence of to the saddle point of the Müller-Brown potential. The present method using a $P+1=4$ point spline is compared to the nudged elastic band (NEB) and growing string (GS) methods (data on the latter two methods are taken from Ref. 30 for comparison).

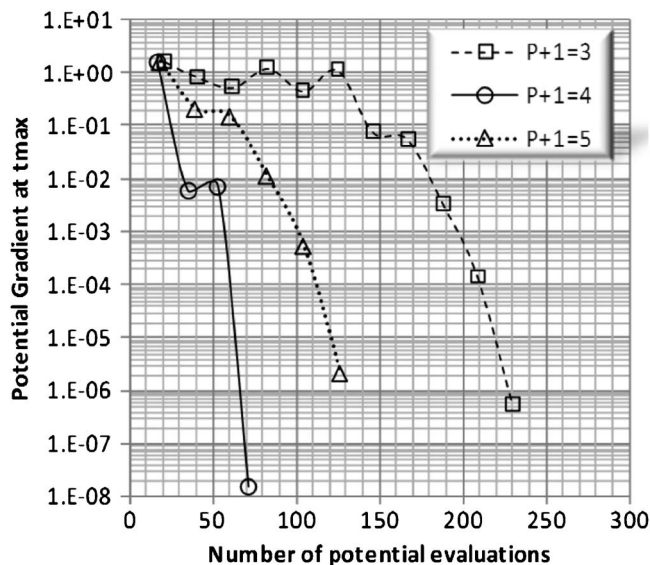


FIG. 4. Convergence to the saddle point of the LEPS potential (measured by the size of the potential surface gradient) vs the number of potential evaluations.

B. The LEPS-type potential

The next example is again a two-dimensional benchmark based on the LEPS potential and developed by Jonsson *et al.*⁴⁹ As seen in Fig. 5 this potential has two minima: The lower minimum is at $r_1=(0.741\ 52, 1.303\ 42)$ with $V_{\min}=-4.509$ and the next minimum is at $r_2=(3.001\ 28, -1.304\ 34)$ with $V_{\min}=-2.620$. Our method starts with a simple approximation, which in our case is a straight line connecting the minima. We use the simplest possible spline, having $P+1=3$ anchor points, i.e., only one anchor point is free to move. Because this is a simple problem, this should suffice. However, it is our experience that using very few points can lead to excessive iterations. We compare the performance of $P+1=3, 4$, and 5 anchor point splines in Fig. 4.

The most obvious feature we find is that the actual amount of work is very sensitive to the number of anchor points. The form of these splines is shown in Fig. 5. These splines depict very different paths but they intersect at the saddle point. In general, as the number of anchor points is increased, the path is also more elaborate.

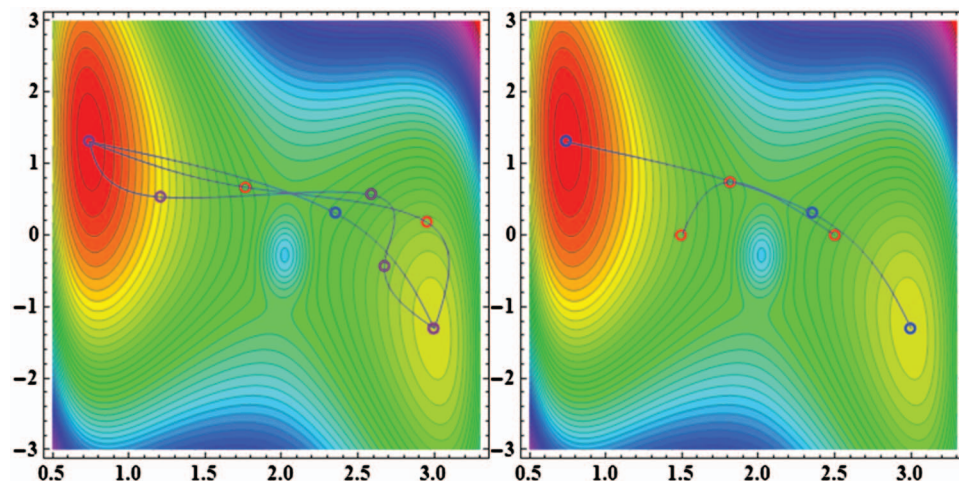


FIG. 5. (Color) Left: Three splines, with $P+1=3, 4$, and 5 anchor points, for finding the saddle point. Right: Two optimized $P+1=3$ splines with different initial and final anchor points.

It may seem that increasing the number of anchor points will allow faster convergence because of increased flexibility. But this is not necessarily so. The reason is that, besides the need to evaluate the potential at more points, the surplus flexibility of the spline tends to increase the number of minimization steps. One should strive to incorporate additional information to reduce the numerical effort. For example, if the initial and final points of the spline are taken closer to the saddle point, for example, at $q_0=(2.5, 0)$ and $q_2=(1.5, 0)$ one still converges to the saddle point as before but with about half the amount of numerical work [see Fig. 5 (right)].

C. Planar Lennard-Jones cluster

This example, taken from Dellago *et al.*,³³ involves 14 dimensions. The system is a planar cluster of seven particles with a potential energy given by the sum of the pair interactions $V=\sum_{i<j}v(|\mathbf{r}_i-\mathbf{r}_j|)$, where the pair potential is the Lennard-Jones (LJ) potential $v(r)=4[r^{-12}-r^{-6}]$. The initial and final configurations are hexagonal shaped clusters (see Fig. 8) with nearest neighbor distances that can be determined analytically to be: $r_0=(11952857/6105888)^{1/6} \approx 1.11846006394$.

We start by running a $P+1=3$ spline. The minimization is quickly seen to yield a maximal energy that oscillates between two values around the value of -10 energy units. This occurs because the spline encounters two identical barriers and being short of anchor points it is unable to optimize one without the other increasing. This is a typical problem when there are not enough anchor points. In spite of this failure, the resulting spline can serve as a good guess for a $P+1=4$ spline. Indeed, the situation improves somewhat: The minimization still fails but now the oscillation takes place between two values close to -10.7 energy units. We further increase the number of anchor points to $P+1=6$ and also tested the cases of $P+1=7$ and $P+1=8$. This time the minimization process converges (see Fig. 6) and the energy along the spline is shown in Fig. 7. The saddle point energy is $-10.798\ 746$. The energy of the endpoints is $-149\ 827\ 467/11\ 952\ 857 = -12.534\ 867$, so the barrier height is $1.736\ 121$. The saddle point energy is converged to these digits. To check stability, we tried other initial guesses (random). In all cases, we con-

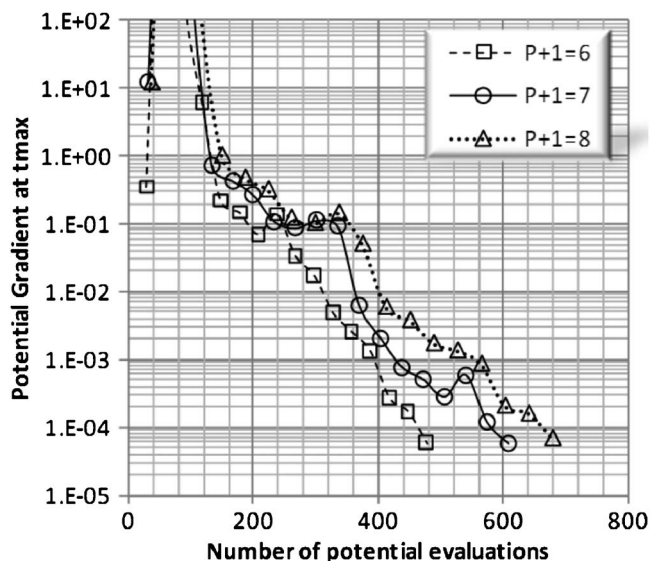


FIG. 6. Convergence to the saddle point of the planar Lennard-Jones cluster (measured by the size of the potential surface gradient) vs the number of potential evaluations.

verge to the same saddle point, even though the splines are somewhat different. This is seen in Fig. 7, where we see the same saddle point energy (although it appears at different values of the parameter t). The saddle point configuration is the same in all cases and it is shown in Fig. 8, along with the initial and final states.

The work needed to reach the saddle point in this 14-dimensional space is about 500–600 energy calls. This is about five to six times larger than the two-dimensional (2D) examples considered above. This shows that, in terms of the number of energy calls, the method scales gently (approximately linearly) with the number of dimensions.

D. Self-diffusion in diamond

In order to study the performance of our method for larger systems, we examine the problem of self-diffusion in a diamond cluster. Carbon atom mobility in diamond is important for diamond growth in thin single-crystal films⁵⁰ and is

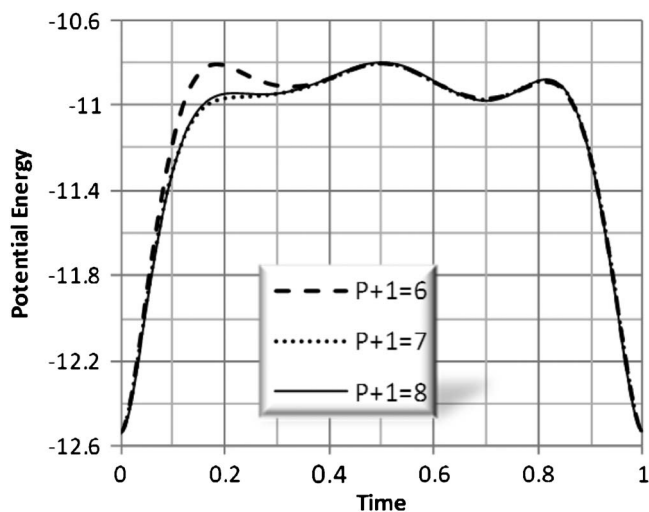


FIG. 7. The potential energy along the three splines (see text).

important for the understanding of self-diffusion in other tetrahedral crystals such as Si.⁵¹ Several conceptual mechanisms involve the existence of defects such as interstitials, vacancies, substitution atoms, etc. However, self-diffusion can also happen in a perfect lattice via a concerted exchange mechanism, as was studied in Si.⁵¹ An *ab initio* investigation of such a self-diffusion mechanism in diamond found a large activation energy of over 13 eV.⁵² Motivated by these studies, we applied our method to find the transition state for concerted exchange in a diamond cluster involving 56 carbon atoms. The surface atoms of the cluster were saturated by 78 hydrogen atoms. The electronic structure and nuclear interactions are described using a tight binding method.⁵³

In Fig. 9 (left), we show the two exchanging atoms and their six nearest neighboring atoms bonded in *sp*³ hybridization. The C–C bond length calculated with the tight binding method is 1.6 Å, slightly longer than the experimental value. This configuration is the initial state. The final state has the same structure, except the two atoms have exchanged.

The initial guess for the spline passing near the saddle point was constructed from the configurations of the concerted exchange mechanism.⁵¹ We fed this path into the algorithm allowing all carbon atoms to move during the search for the saddle point. However, the algorithm converged extremely slowly. Thus, we decided to try another approach composed of two stages. In the first stage, we froze all atoms of the cluster except for the two exchanging atoms and their six nearest neighbors. This 24 degrees of freedom (DOFs) saddle search converged well within about 1300 iterations (see Fig. 10). The saddle point searches involved splines with $P+1=6$ anchor points and the convergence criterion was a gradient of 10^{-6} per DOF. The converged transition state shows a planar structure with activation energy of 15.7 eV. In the second stage we used the converged spline as the initial guess for a new saddle point search where all 56 carbon atoms were allowed to move. The number of potential evaluations for the second 168 DOF stage is also about 1300.

The saddle point shows a coplanar ethylene like structure (see Fig. 9, right) with the exchanging atoms exhibiting double bond character (distance of ~ 1.3 Å) and *sp*² bonding (angle of 122°) with their neighbors. This transition state has an activation energy of 12.8 eV, showing that almost 3 eV are associated with lattice relaxation, beyond the immediate neighborhood of the exchanging atoms. This barrier height is similar to the value of 13.2 eV reported for the *ab initio* calculation.⁵²

The initial guess we supplied, based on the mechanism suggested for Si,⁵¹ turned out to be problematic. This is the reason for the nonmonotonic convergence pattern seen for the first stage (24 DOFs) in Fig. 10. Indeed, the final saddle point we found for the diamond cluster is *not* the configuration suggested for the Si crystal. Even with this relatively poor initial guess, the algorithm performed reasonably well.

V. CONSTRAINED MINIMIZATION

The saddle point search algorithm can also be used to search for constrained minimization solutions. We raise this

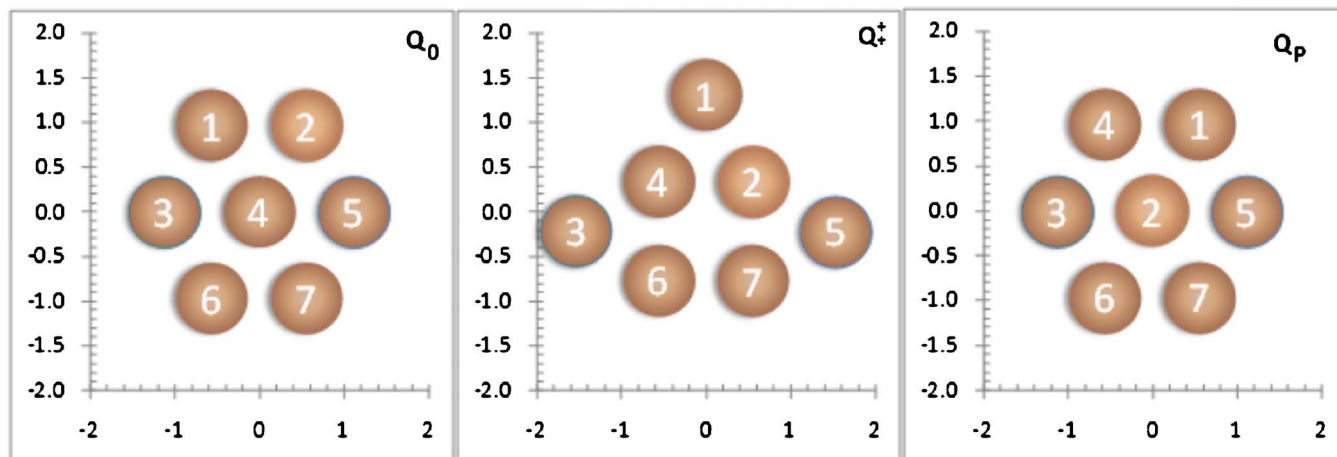


FIG. 8. (Color online) The initial (Q_0), saddle point (Q^*) and final (Q_p) configuration of the MEP. The same saddle point configuration is obtained for the two splines.

issue for two purposes. First, we want to check what happens when the number of dimensions in the hypersurface grows. Constrained minimization problems are easy to invent and solve analytically. Second, many self-consistent field approaches in quantum chemistry and statistical physics involve constrained minimization.

A constrained minimization problem is stated as

$$\text{minimize } f(\mathbf{x})$$

$$\text{subject to } \mathbf{h}(\mathbf{x}) = 0. \quad (5.1)$$

Here, $\mathbf{x} \in \mathcal{R}^N$ is a N -dimensional vector, and $\mathbf{h}(\mathbf{x})$ are M equality constraints. This problem can be solved once a saddle point is located for the function

$$L(\mathbf{x}, \mathbf{a}) = f(\mathbf{x}) - \mathbf{a} \cdot \mathbf{h}(\mathbf{x}). \quad (5.2)$$

$\mathbf{a} \in \mathcal{R}^M$ are M Lagrange multipliers.⁴² The saddle point we seek is built such that the function is a maximum in directions contained in the \mathbf{a} space (holding \mathbf{x}) and a minimum in directions contained in the \mathbf{x} space (holding \mathbf{a}). Thus, instead of minimizing the function $f(\mathbf{x})$, one can find the saddle point of $L(\mathbf{x}, \mathbf{a})$, considered as a function of $N+M$ variables.

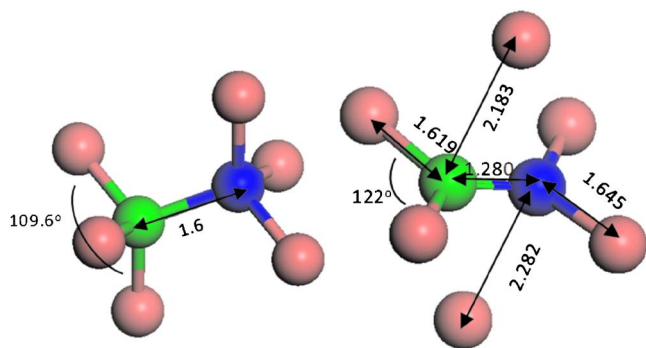


FIG. 9. (Color online) A close-up view of two carbon atoms involved in direct exchange along with their nearest neighbors. Left: The initial configuration in the relaxed diamond and right: The saddle point configuration. Bond lengths are in ångströms. The saddle-point structure was calculated when all 56 carbon atoms were allowed to relax.

As a warm up, let us consider the following trivial example:

$$\text{minimize } x^2$$

$$\text{subject to } x - 1 = 0. \quad (5.3)$$

It is obvious that the constrained minimum is at $x=1$ and the value of $f(x)$ is 1. The saddle point formalism does not know that this problem is trivial. The Lagrangian is

$$L(x, a) = x^2 - a(x - 1), \quad (5.4)$$

as plotted in Fig. 11. Before searching for a saddle point, we need to determine an initial and a final point of the path. This is easily done by setting a point \tilde{x}_0 for which $h(\tilde{x}_0) > 0$ and a negative \tilde{a}_0 and then repeatedly stepping down a descent direction until reaching (x_0, a_0) , where L is smaller than the estimated height of the saddle point. The same is done for x_f [but taking $h(\tilde{x}_f) < 0$ and $\tilde{a}_f > 0$]. Once the endpoints are set, we use a $P+1=3$ anchor point spline (two points are fixed at

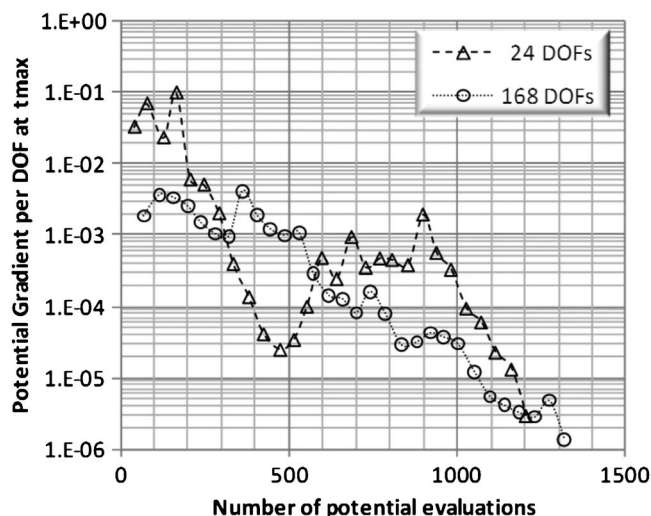


FIG. 10. The norm of the PES gradient per DOF vs number of potential evaluations during the saddle point search for the concerted exchange reaction in the diamond cluster. The two stages shown are the 8-mobile carbon atom (24 DOFs) and the 56 mobile carbon atom search (168 DOFs).

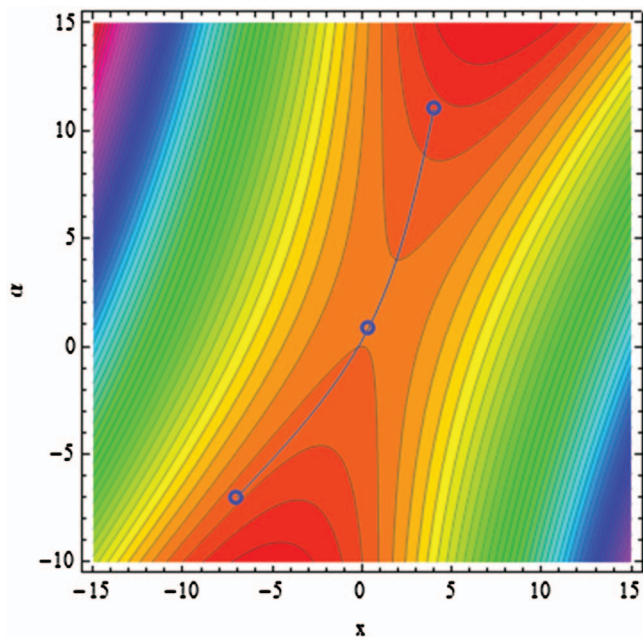


FIG. 11. (Color) A contour plot of the Lagrangian in Eq. (5.4). We depict a spline used to locate the saddle point. The blue circles denote the position of the $P+1=3$ anchor points.

the endpoints and thus only the middle point is free to move). The search for the saddle-point using our program takes four LBFGS iterations and involves 70 $L(x, a)$ evaluations. The saddle point is determined to be at $(x, a) = (1, 2)$, and the function value is $L(1, 2) = 1^2 = 1$. The accuracy of the algorithm allows finding the minimum accurate to 11 digits. The minimizing spline is shown in Fig. 11.

As a last example, we want to study a multidimensional saddle point problem. Our purpose is to demonstrate the behavior of the algorithm as the scaling of the system grows. Consider the minimization problem,

$$\begin{aligned} \text{minimize} \quad & e^{(1/2\sigma^2)x^T x} + q^T x \\ \text{subject to} \quad & r^T x = b, \end{aligned} \quad (5.5)$$

where x , q , and r are real vectors of dimension N . This is an example for which the saddle point search involves $N+1$ variables. Thus, we can get a sense of the behavior of the saddle point search method for many DOFs. For simplicity, let us also require that r and q are orthogonal, $r^T q = 0$ (in the applications below, q and r are selected at random and then r is orthogonalized).

This problem becomes a search for a saddle point of the functional

$$L(x, a) = e^{(1/2\sigma^2)x^T x} + q^T x - a(r^T x - b). \quad (5.6)$$

We chose a simple enough problem so that there is a tractable analytical solution. We give this solution in the Appendix. The examples below uses $\sigma=1$, random vectors for r and q , and a random number between 0 and 1 for b .

We have repeated the saddle search associated with Eq. (5.6) for increasingly large values of $N=10, 100$, and 1000. We find the number of iterations and function evaluations almost independent of system size. At $N=10$,

there are 125 function evaluations, at $N=100, 161$, and at $N=1000, 185$. Since each Lagrangian evaluation takes $O(N)$ operations, the saddle search is *linear in system size*. There are also a few gradient evaluations (about 5% of the Lagrangian evaluations). In general, gradient evaluations will scale quadratically for N -dimensional problems. However, in many applications, as, for example, in linear-scaling electronic structure,^{43,54–57} they can be made to scale linearly as well. Thus, this result is indicative that this saddle point method may be useful for order- N electronic structure calculations.

VI. SUMMARY

In this paper, we presented a straightforward method to find the saddle point, be it the transition state of a potential hypersurface or a solution of a constrained minimization problem. The use of splines is the important element. This allows us to start with a path between known initial and final states (reactants and products) and to find a relevant saddle point between them. The splines we use are cubic splines having second order smoothness. This is required for the efficiency of the saddle search.

The results we find are very encouraging since in all cases we were able to converge to the saddle point with extremely high accuracy and efficiency (small number of anchor points). The combination of spline stiffness and flexibility allows finding solutions in multidimensional problems such as the 2D Lennard-Jones cluster (14 DOFs), the 56 carbon atom cluster (168 DOFs), and the 10^3 DOFs in the constrained minimization problems.

Once the saddle point is determined at high accuracy, the minimum energy path can be constructed by standard methods developed for this purpose.^{15,16} In some cases this may require some Hessian evaluations.

We have also studied a saddle point problem of constrained minimization, which has many chemical applications in quantum chemistry and statistical physics. While we have not compared to other methods, we found initial indications that the present method allows an efficient minimization which is linear with the number of DOFs. In the constrained minimization problem, the constraints are inserted with additional variables (the Lagrange multipliers) coming in linearly. The same idea can be used for adding constraints into the transition state search. This and other issues, such as the incorporation of the present algorithm into a quantum chemistry code, are deferred to later studies.

ACKNOWLEDGMENTS

This research was funded by the Israel Science Foundation (ISF).

APPENDIX: ANALYTICAL SOLUTION OF THE CONSTRAINED MINIMIZATION EXAMPLE

In this appendix we simply state the analytical solution of the constrained minimization problem setup in Sec. V [Eq. (5.5)] and described as a saddle point problem [Eq. (5.6)]. Because of the constraint $r^T q = 0$, the optimal x_* is a linear combination of q and r , which we

write as $(1/\sigma^2)x_* = (b/\sigma_r^2)r + (c/\sigma_q^2)q$, where $\sigma_r^2 = (r^T r)\sigma^2$ and $\sigma_q^2 = (q^T q)\sigma^2$. The only unknown is the number c and it can be obtained by solving the equation

$$\frac{c}{\sigma_q} \exp\left(\frac{c^2}{2\sigma_q^2}\right) = -\sigma_q \exp\left(-\frac{b^2}{2\sigma_r^2}\right). \quad (\text{A1})$$

This shows that c is negative. Equation (A1) can be solved by a few Newton–Raphson iterations. The optimal Lagrange multiplier is $a_* = -(\sigma_q^2 b)/(\sigma_r^2 c)$. The constrained minimal value is given by $L(x_*, a_*) = c - \sigma_q^2/c$.

¹M. Baer, *Theory of chemical reaction dynamics* (CRC, Boca Raton, FL, 1985).

²M. A. Collins, *Adv. Chem. Phys.* **93**, 389 (1996).

³M. G. Evans and M. Polyani, *Trans. Faraday Soc.* **31**, 875 (1935).

⁴H. Eyring, *J. Chem. Phys.* **3**, 107 (1935).

⁵R. D. Levine and R. B. Bernstein, *Molecular Reaction Dynamics and Chemical Reactivity* (Oxford University Press, Oxford, 1987).

⁶D. G. Truhlar, A. D. Issacson, and B. C. Garrett, in *Theory of Chemical Reaction Dynamics*, edited by M. Baer (CRC, Boca Raton, FL, 1985), Vol. 4, p. 65.

⁷W. H. Miller, *J. Chem. Phys.* **61**, 1823 (1974).

⁸D. Chandler, *J. Chem. Phys.* **68**, 2959 (1978).

⁹J. T. Hynes, in *Theory of Chemical Reaction Dynamics*, edited by M. Baer (CRC, Boca Raton, FL, 1985), Vol. 4, p. 65.

¹⁰E. A. Carter, G. Ciccotti, J. T. Hynes, and R. Kapral, *Chem. Phys. Lett.* **156**, 472 (1989).

¹¹G. L. Hofacker, *Z. Naturforsch. A* **18**, 607 (1963).

¹²R. A. Marcus, *J. Chem. Phys.* **45**, 4500 (1966).

¹³K. Fukui, *J. Phys. Chem.* **74**, 4161 (1970).

¹⁴W. H. Miller, N. C. Handy, and J. E. Adams, *J. Chem. Phys.* **72**, 99 (1980).

¹⁵C. Gonzalez and H. B. Schlegel, *J. Chem. Phys.* **90**, 2154 (1989).

¹⁶M. Page, C. Doubleday, and J. W. Mciver, *J. Chem. Phys.* **93**, 5634 (1990).

¹⁷J. E. Sinclair and R. Fletcher, *J. Phys. C* **7**, 864 (1974).

¹⁸C. J. Cerjan and W. H. Miller, *J. Chem. Phys.* **75**, 2800 (1981).

¹⁹M. J. Rothman and L. L. Lohr, *Chem. Phys. Lett.* **70**, 405 (1980).

²⁰S. Bell and J. S. Crighton, *J. Chem. Phys.* **80**, 2464 (1984).

²¹V. I. Irina and A. C. Emily, *J. Chem. Phys.* **98**, 6377 (1993).

²²W. Quapp, M. Hirsch, O. Imig, and D. Heidrich, *J. Comput. Chem.* **19**, 1087 (1998).

²³I. V. Ionova and E. A. Carter, *J. Chem. Phys.* **98**, 6377 (1993).

²⁴L. R. Pratt, *J. Chem. Phys.* **85**, 5045 (1986).

²⁵R. Elber and M. Karplus, *Chem. Phys. Lett.* **139**, 375 (1987).

²⁶A. Ulitsky and R. Elber, *J. Chem. Phys.* **92**, 1510 (1990).

²⁷S. Fischer and M. Karplus, *Chem. Phys. Lett.* **194**, 252 (1992).

²⁸G. Mills and H. Jonsson, *Phys. Rev. Lett.* **72**, 1124 (1994).

²⁹R. Olender and R. Elber, *J. Chem. Phys.* **105**, 9299 (1996).

³⁰B. Peters, A. Heyden, A. T. Bell, and A. Chakraborty, *J. Chem. Phys.* **120**, 7877 (2004).

³¹S. K. Burger and W. T. Yang, *J. Chem. Phys.* **124**, 054109 (2006).

³²D. Passerone and M. Parrinello, *Phys. Rev. Lett.* **87**, 108302 (2001).

³³C. Dellago, P. G. Bolhuis, and D. Chandler, *J. Chem. Phys.* **108**, 9236 (1998).

³⁴F. Jensen, *J. Chem. Phys.* **102**, 6706 (1995).

³⁵H. Jonsson, G. Mills, and K. W. Jacobsen, in *Classical & Quantum Dynamics in Condensed Phase Simulations*, edited by B. J. Berne (World Scientific, Singapore, 1998), pp. 385.

³⁶G. Henkelman, G. Johansson, and H. Jonsson, in *Progress on Theoretical Chemistry and Physics*, edited by S. D. Schwartz (Kluwer Academic, Dordrecht, 2000), pp. 269.

³⁷E. Weinan, R. Weiqing, and V.-E. Eric, *Phys. Rev. B* **66**, 052301 (2002).

³⁸W. Quapp, *J. Comput. Chem.* **28**, 1834 (2007).

³⁹W. Quapp, *J. Comput. Chem.* **25**, 1277 (2004).

⁴⁰G. Henkelman and H. Jonsson, *J. Chem. Phys.* **113**, 9978 (2000).

⁴¹D. Chandler, in *Classical and Quantum Dynamics in Condensed Phase Simulations*, edited by B. J. Berne, G. Ciccotti, and D. F. Coker (World Scientific, Singapore, 1998), p. 51.

⁴²P. Gill, *Practical Optimization* (Academic, New York, 1982).

⁴³S. Adhikari and R. Baer, *J. Chem. Phys.* **115**, 11 (2001).

⁴⁴D. Wales, *Energy Landscapes: Applications to Clusters, Biomolecules and Glasses* [Cambridge University Press, Cambridge, 2003].

⁴⁵C. De Boer, *A Practical Guide to Splines*, 2nd ed. (Springer, New York, 2000).

⁴⁶W. H. Press, S. A. Teukolsky, W. T. Vetterling, and B. P. Flannery, *Numerical Recipes in C* (Cambridge University Press, Cambridge, 1992).

⁴⁷D. C. Liu and J. Nocedal, *Math. Program.* **45**, 503 (1989).

⁴⁸K. Muller and L. D. Brown, *Theor. Chim. Acta* **53**, 75 (1979).

⁴⁹H. Jonsson, G. Mills, and K. W. Jacobson, in *Classical and Quantum Dynamics in Condensed Phase Simulations*, edited by B. J. Berne, G. Ciccotti, and D. F. Coker (World Scientific, Singapore, 1998), p. 385.

⁵⁰M. N. R. Ashfold, P. W. May, C. A. Rego, and N. M. Everitt, *Chem. Soc. Rev.* **23**, 21 (1994).

⁵¹K. C. Pandey, *Phys. Rev. Lett.* **57**, 2287 (1986).

⁵²J. Bernholc, A. Antonelli, T. M. Delsole, Y. Baryam, and S. T. Pantelides, *Phys. Rev. Lett.* **61**, 2689 (1988).

⁵³Y. Wang and C. H. Mak, *Chem. Phys. Lett.* **235**, 37 (1995).

⁵⁴R. Baer and M. Head-Gordon, *Phys. Rev. Lett.* **79**, 3962 (1997).

⁵⁵S. Goedecker, *Rev. Mod. Phys.* **71**, 1085 (1999).

⁵⁶R. Baer and M. Head-Gordon, *Phys. Rev. B* **58**, 15296 (1998).

⁵⁷W. Z. Liang, C. Saravanan, Y. H. Shao, R. Baer, A. T. Bell, and M. Head-Gordon, *J. Chem. Phys.* **119**, 4117 (2003).